Tillage Quality Measurement: Surface Roughness Analysis using Height Profiles

M. Sc. **M. Graf**, AGCO GmbH, Marktoberdorf;
Prof. Dr.-Ing. **M. Geimer**, Karlsruhe Institute of Technology, Karlsruhe

Abstract

Surface roughness is a critical factor during the tillage process, as it impacts soil erosion, hydrological mechanisms, and seedbed preparation. However, surface roughness can be described using various parameters, such as root mean square height or mean upslope depression index, which complicates the selection of the most appropriate parameter for measuring tillage process quality. This paper presents an approach to determine the most relevant parameters for measuring surface roughness for the tillage process with a cultivator. The approach consists of three steps. First, surface height profiles are generated in a simulation environment. Second, we evaluate different roughness parameters and analyze them using Spearman's rank correlation coefficient. The analysis results in parameter clusters that exhibit similar correlations and thus likely describe similar physical properties. Based on this classification, appropriate parameters are selected. Finally, we compare the simulation environment's correlation matrix with the field trial data correlation matrix. The results indicate that Rq_x, Rq_y, and Sq are the best parameters for characterizing surface roughness at the aggregate level during tillage with a cultivator. These parameters are computationally efficient and provide comprehensive information about the roughness for slope- and anomaly-free data.

Introduction

The tillage tasks, objectives, and implements vary throughout the year, depending on the crop rotation. Machinery and Equipment Manufacturers Association (VDMA) Agricultural Machinery and Bavaria's Farmers' Association suggests in [1] that the next steps to enhance automation in tillage include implementing assistance systems, automatic control, and documentation of subtasks according to the farmer's specification. Consequently, a monitoring system is required to assist and document the process. This system can also measure the process outcome, which we define as process quality in this paper. One potential quality parameter for the tillage process with a cultivator is the roughness of the soil surface. An even, homogenous seedbed ground is necessary for uniform crop germination and growth. Also, surface roughness affects soil erosion and hydrological processes [2].

Most parameters describing surface roughness rely on height profiles, which can be obtained using contact-measurement devices like relief meters ([3]) or non-contact-measurement devices like laser scanners or stereo vision systems (e.g. [4], [5], [6], [7]). Evaluated parameters range from predicting surface storage capacity ([2]) to the standard deviation of individual elevation points ([8]), the index of Currence and Lovely ([9]), and Peak Frequency ([10]).

This paper presents an approach to identify the most relevant roughness parameters from the wide range of potential parameters for the tillage process with a cultivator. The used approach ensures that the parameters are verified under controlled, reproducible conditions.

Related Work

The term surface roughness in agriculture is not as sharply defined as it is in the context of technical surfaces [11]. Römkens and Wang propose in [10] four types of soil surface roughness in their study. The four types are (1) isotropic microrelief variations caused by grains or micro aggregates (~1 mm), (2) isotropic variations caused by soil clods (~100 mm), (3) anisotropic differences due to implement (100…200 mm), (4) higher-order roughness at field or landscape level. Their study focuses on type 2 roughness as it describes the outcome of the tillage process. The effects of implements (type 3) during the measurement are excluded. A similar classification can be found in [11] for the shape deviations of technical surfaces. Type 1 pertains to shape deviations, type 2 to waviness, and type 3 and 4 to periodic or aperiodic roughness. To differentiate between the various types of shape deviations for technical surfaces, DIN EN ISO 25178-2 defines S (short wavelength), L (long wavelength), and F (form shape) filter operations [12]. The analogous concept for profiles can be found in [13]. In the context of soil roughness parameters, e.g., in [2] or [9], the elimination of slope (F operation) is proposed. However, an explicit separation of waviness and roughness is not defined.

A large number of roughness parameters have already been defined and classified in [13] for profiles (*R*-parameters) and in [12] for surfaces (*S*-parameters). The roughness parameter definitions introduced in the agricultural context are aligned with these standards (see Table 1). The specific calculation rules can be found in the indicated references.

In addition to the theoretical considerations, various publications use different sensor technologies for data acquisition to measure process quality. For example, the authors in [4], [6] or [14] measure the *RC* parameter of the surface processed with a rotary harrow using a stereo vision system or infrared distance meter. The authors in [15] use a stereo vision system to determine *Rz*. Steinhaus in [16] uses a laser scanner profile to measure Rq_x.

Table 1: Comparison of the roughness parameters from [12] and [13] and the roughness parameters from the agricultural context

	Roughness Parameters from [12] and [13]		**Parameters in Agriculture Context**	
Amplitude	Arithmetic mean deviation of the height	Ra/Sa	Area between profile and the best-fit line through measurement data	*MI* [10]
	Root mean square height	Rq/Sq	Standard deviation of (logarithmic) heights	*s* /(*RR*) [8]
			Height residuals to best-fitted plane through measurement data	*RC* [9]
	Maximum height of valleys	Rv/Sv		
	Maximum height of peaks	Rp/Sp		
	Maximum height	Rz/Sz		
	Skewness of the height distribution < 0: load-bearing surface	Rsk/Ssk		
	Kurtosis of the height distribution < 3: even height distribution	Rku/Sku		
			Limiting elevation difference	*LD* [17]
Spatial	Autocorrelation length	Sal		
	Texture aspect ratio	Str		
	(Density of peaks)	Spd	Peak frequency	*F* [10]
			Limiting slope	*LS* [17]
Hybrid	Developed interfacial area ratio	Rmr/Sdr	Tortuosity index	*TB* [18], [19]
	Root mean square slope/gradient	Rdq/Sdq		
			Mean Upslope Depression index	*MUD* [2]
			$\sqrt{LD \cdot LS}$	*Q* [20]
			$MI \cdot F$	*MIF* [10]
Func-tional	Parameters of the Abbott curve	Rk/Sk, Rpk/Spk, Rvk/Svk, Mr1/Smr1, Mr2/Smr2		

In [21], the authors use a 2D laser profilometer to measure the surface roughness. They compare the roughness of four/five tillage processes (moldboard plow, harrowed rough, harrowed smooth, planted unmodified (seedbed), planted modified (seedbed + rainfall)). The most sensitive parameters for separating the different process types were *MUD*, and *LD*, and for rainfall, the parameters *LS* and crossover lengths. In [5], the authors evaluate the effectiveness of the terrestrial laser scanner and structure from motion photogrammetry in measuring soil surface roughness (*RR*) across different agricultural soils, comparing these methods with 2D laser profilometer measurements.

Method and Data

This paper follows the proposed method in [22]. Initially, synthetic datasets of surfaces were generated in a deterministic environment. Therefore, surfaces were created with the rendering tool Blender ([20]). The 3D data was generated using Gazebo ([15]) with a mechanical lidar model based on the Ouster OS1 (128 layers with 2048 points per layer). In one approach, the surface was defined by half-spheres, which modeled soil aggregates (see Fig. 1). The simplified assumption is based on the sieve analysis, which can only provide a statistical diameter. This approach focuses on roughness, whereas waviness is omitted. In another approach, different soil aggregates (varying in size and shape) were modeled and distributed on a plane according to the Rosin-Rammler-Sperling-Bennett (RRSB)-distribution [23], [24] (see Fig. 2). The ground plane scenarios include even and wavy surfaces. The waviness is represented by a sinusoidal wave in the direction with the higher resolution (*x*-direction), with its frequency depicting different exemplary scenarios (e.g., tine spacing, disc spacing, or roller profile of an exemplary cultivator). The wave amplitude is half, full, and double the distributed aggregates weighted mean diameter (MWD).

To summarize, the following scenarios are analyzed:

- Half-spheres with diameter *d* = 10, 20, 40, 60, 80 mm (“half-sphere scenario”)
- Deformed spheres with *d* ≈ 10, 20, 40, 80 mm, distributed according to RRSB, on sinusoidal wave planes with amplitudes $a = [0, 0.5 , 1, 2] * MWD$ and frequencies *f* = 2.5, 3.6, 7.9 Hz (“statistical scenario”)

In the second step, the parameters from Table 1 were implemented and tested on the datasets. The results underwent statistical evaluation using Spearman's rank correlation coefficient to find parameters that describe the same physical properties and detect parameters with unique significance. Spearman’s rank correlation coefficient is more robust against outliers than the Pearson correlation coefficient and, therefore, preferred [20].

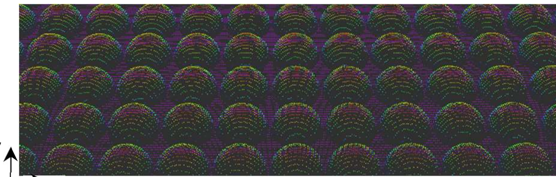

Fig. 1: Half-sphere scenario

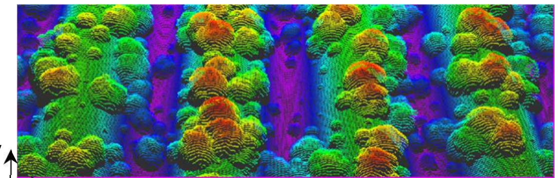

Fig. 2: Statistical scenario (MWD = a = 38 mm, f = 3.6 Hz)

In the third step, the parameter set was reduced to parameters that probably describe different physical properties. The parameter correlations were validated using data from field trials. The exemplary data for sandy, loamy, and peaty soils were recorded in 2023 and 2024 during primary tillage using a 3 m cultivator with a cage roller. The lidar sensor (Ouster OS1) was mounted behind the roller.

Results

Fig. 3 visualizes the correlation matrices of the implemented roughness parameters in the half-sphere scenario (bottom left) and the statistical scenario (top right). Very strong correlations ($r_S = \pm(0.8 \dots 1.0)$) are visualized using red/purple and blue/green, with red/purple indicating positive correlations and blue/green indicating negative correlations. Weaker correlations are represented with more transparent colors. No statistically significant correlations (p-values higher than 0.05) are marked with a cross. The profile parameters can be evaluated in two directions and are listed with index *x* and *y* (R_x/R_y). The *x*-direction corresponds to the direction with higher resolution and is the direction of the waves (see Fig. 2) or vertical to the direction of travel for the field trial data.

The key findings are described in the following. The height parameters of the amplitude parameters cluster, *Ra/Sa, MI, Rq/Sq, Rp/Sp, Rv/Sv,* and *Rz/Sz,* correlate very strongly with each other. *LD*'s correlation to these parameters is moderate to strong in the half-sphere scenario. LD_x behaves similarly in the context of the statistical scenario, while LD_y only has a weak correlation. The parameters *Rsk*/*Ssk* and *Rku*/*Sku* describe information about the surface shape (load-bearing capacity/profile peak ratio or flattened peaks and valleys). Rsk_x shows a non-statistical correlation with the height parameters in the half-sphere scenario. In the statistical scenario, the *x* components of *Rsk* and *Rku* correlate very strongly to the height parameters, and the *y* components weakly. Parameter *Ssk* correlates strongly negatively, and *Sku* weakly or not statistically significant.

Regarding *Sal*, one parameter of the spatial parameters cluster, there is a strong correlation between this and all other parameters in the context of the half-sphere scenario. The statistical scenario shows only very weak correlations. *Str* demonstrates a strong correlation with all parameters in both scenarios. However, no statistically significant correlation was observed between *Str* and the hybrid parameters in the half-sphere scenario. The correlation between F_x and F_y and all other parameters is strong, except Rsk_x and MUD_{DSC} in the half-sphere scenario. A weak correlation between F_x and LD_y, Rsk_y, Rku_x, *Sku,* and LS_y is shown in the statistical scenario. F_y shows only a moderate to strong correlation with Rsk_y, Rku_y, and *Sku*. The correlation between *LS* and the amplitude parameters is stronger in the half-sphere scenario than in the statistical scenario.

The hybrid parameter cluster shows weaker correlations to the height parameters in the half-sphere scenario than in the statistical scenario. Parameter MUD_{DSC} demonstrates a weak negative correlation in the half-sphere scenario. Except for *Str,* the correlation between the hybrid and spatial parameters is moderate to strong in the half-sphere scenario. Only *Str*, F_y, and *LS* show a strong correlation in the statistical scenario.

In the half-sphere scenario, the functional and height parameters are strongly correlated. In the statistical scenario, the correlation is moderate to strong. The hybrid parameters correlate moderately to strongly with the functional parameters in both scenarios.

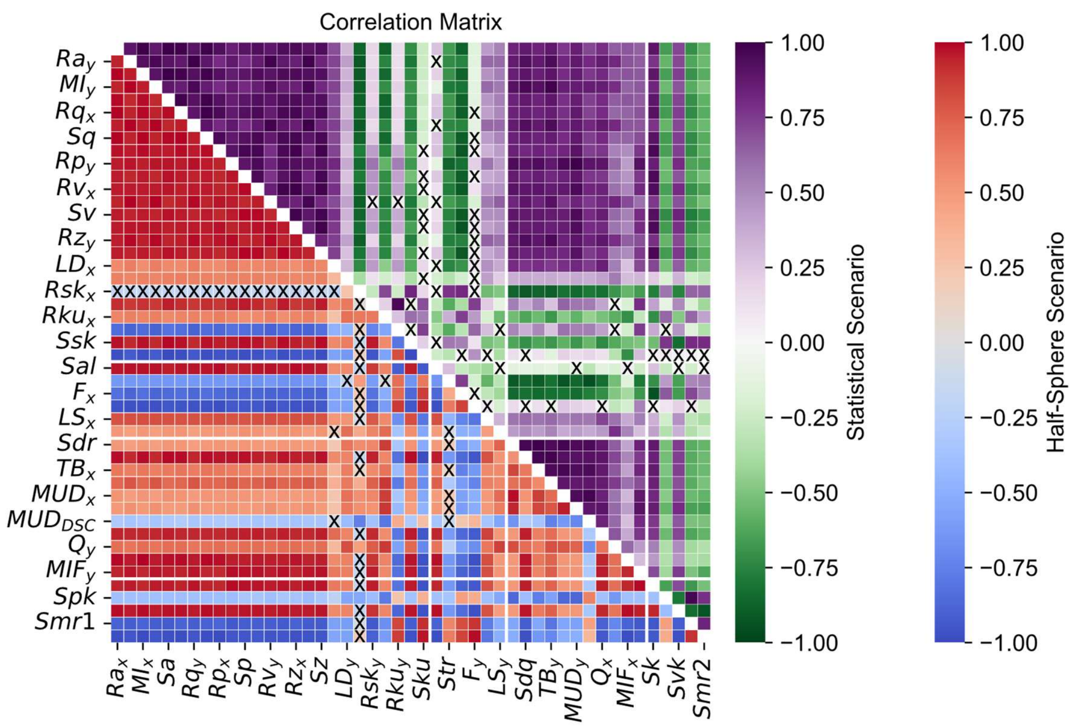

Fig. 3: Correlation matrices of potential roughness parameters (synthetic data)

Discussion

The height parameters, *Ra, Ml, Rq, Rp, Rv,* and *Rz,* strongly correlate. However, the correlation between the *x* and *y* components of the parameters is reduced in the statistical scenario compared to the half-sphere scenario. The *x* and *y* components in the statistical scenario evaluate different characteristics (waviness in the *x*-direction, roughness in the *y*-direction). It is, therefore, useful to evaluate the parameters separately in the *x* and *y* directions in addition to a generalizing surface parameter such as *Sq*. The authors of this paper propose focusing on Rq_x, Rq_y, and *Sq* for the height parameter cluster due to the straightforward calculation and outlier weighting.

The *LD, LS,* and *Q* parameters correlate moderately to the height parameters. *LS* is the inverse of the slope of the regression line through the measured data points. Lines with nearly zero slope and thus division near zero produce outliers. *LD*, as the inverse of the intercept, shows more robustness. Nevertheless, this point is less critical for uneven data like the statistical scenario.

Theoretically, *Rsk/Ssk* and *Rku/Sku* should remain constant across the half-sphere scenario. Resolution inaccuracies probably lead to the evaluated correlation. *Sal, Sdq, Sdr* and *TB* evaluate the fineness of the measured surface. The algorithm for *Sal* depends on a threshold that can be adjusted, resulting in varying outcomes. *Sdr* and *TB* parameter values increase for rough and fine surfaces, resulting in inconsistent behavior concerning roughness on an aggregate level. The elevation differences between a reference point and another point upslope along a line segment determine the *MUD*. This results in a tendency to evaluate the slope/waviness rather than the roughness on the aggregate level. Therefore, the correlation values between *MUD* and the other parameters are higher in the statistical scenarios.

The functional parameters indicate a moderate to very strong correlation across nearly all parameters. Given the considerable computational burden associated with their specialized nature, further analysis is omitted.

Fig. 4 visualizes the correlation matrices of the statistical scenario (bottom left) and field trial data (top right). The parameters are reduced to those with a unique and statistically significant behavior in the deterministic environment. The field trial data has been corrected using a RANSAC-fitted plane to eliminate the slope, vibrations, and movement of the mobile measurement setup. The correlations are less intense in the field trial data than those observed in the synthetic data. The height parameters *Rq*/*Sq* correlate strongly with each other. The correlation between *LD* and *LS* with the height parameters is very weak; for *Q*, it is moderate. *MUD*'s correlation with the height parameter is strong, while the correlation between MUD_{DSC} and all other parameters is very weak to weak or not statistically significant. The correlation behavior of *Sku* differs from the statistical scenario. *Sdr* and *Sdq* correlate strongly with the height parameters, the *Q* parameters, and the *MUD* parameters. The correlation with the *LD* parameters is very weak to weak.

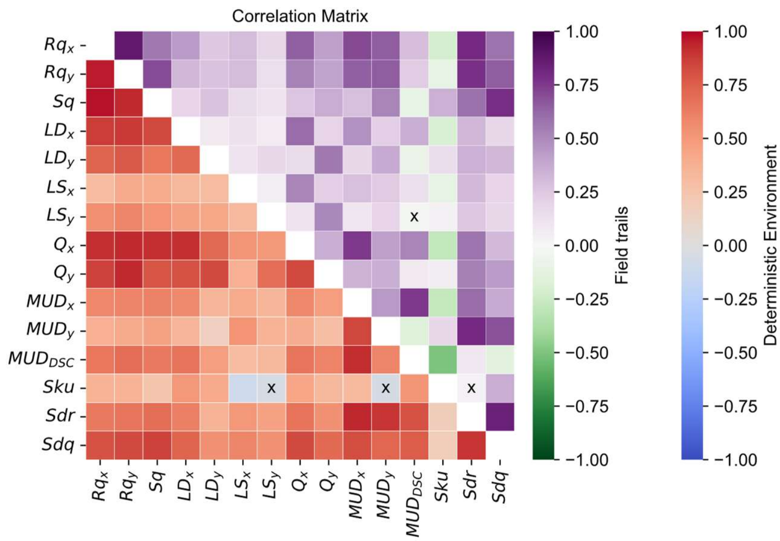

Fig. 4: Correlation matrix of roughness parameters (synthetic and field trial data)

Conclusion and Outlook

The results indicate that evaluating profile parameters, in addition to a surface parameter, provides comprehensive information about the roughness on the aggregate level. Apart from the *LD*, *LS,* and MUD_{DSC} parameters, the other roughness parameters correlate with the height parameters Rq_x, Rq_y, and *Sq* in both deterministic environment scenarios and on field trail data. Accordingly, the authors recommend using these more straightforward parameters concerning computational efficiency.

Further investigations are necessary regarding filtering. Currently, the data is corrected using a RANSAC plane fitting algorithm, avoiding anomalies/waviness. For example, a bandpass filter should be examined more closely to separate roughness on the aggregate level from waviness.

The field trial dataset was recorded using a cultivator with one roller type, whereas the roller type significantly affects the roughness. Testing the method on data from different roller types and the plowing or rotary harrowing process would also be worthwhile. To enhance the statistical significance of this analysis, additional data of varying tillage processes and soil types should be considered.

References

[1] Verein Deutscher Maschinen und Anlagen (VDMA) Landtechink and Bayerischer Bauernverband, “Digital erfolgreich werden: Betriebs-Check und Planungshilfe für Praktiker,” Oct. 2020. [Online]. Available: https://www.vdma.org/documents/34570/040eb2e2-8921-89c0-ef75-2e887509ce5f

[2] B. Hansen, P. Schjønning, and E. Sibbesen, “Roughness indices for estimation of depression storage capacity of tilled soil surfaces,” *Soil Tillage Res.*, vol. 52, no. 1–2, pp. 103–111, Jan. 1999, doi: 10.1016/S0167-1987(99)00061-6.

[3] H. Kuipers, “A reliefmeter for soil cultivation studies.,” *Neth. J. Agric. Sci.*, vol. 5, no. 4, Art. no. 4, Nov. 1957, doi: 10.18174/njas.v5i4.17727.

[4] J. Boysen, L. Zender, and A. Stein, “Modeling the soil-machine response of secondary tillage: A deep learning approach,” *Smart Agric. Technol.*, vol. 6, p. 100363, Dec. 2023, doi: 10.1016/j.atech.2023.100363.

[5] A. Martinez-Agirre *et al.*, “Evaluation of Terrestrial Laser Scanner and Structure from Motion photogrammetry techniques for quantifying soil surface roughness parameters over agricultural soils,” *Earth Surf. Process. Landf.*, vol. 45, no. 3, pp. 605–621, Mar. 2020, doi: 10.1002/esp.4758.

[6] P. Riegler-Nurscher *et al.*, “A system for online control of a rotary harrow using soil roughness detection based on stereo vision,” in *Land.Technik AgEng 2017*, VDI Verlag, 2017, pp. 559–566. doi: 10.51202/9783181023006-559.

[7] L. M. Thomsen, J. E. M. Baartman, R. J. Barneveld, T. Starkloff, and J. Stolte, “Soil surface roughness: comparing old and new measuring methods and application in a soil erosion model,” *SOIL*, vol. 1, no. 1, pp. 399–410, Apr. 2015, doi: 10.5194/soil-1-399-2015.

[8] R. R. Allmaras, *Total Porosity and Random Roughness of the Interrow Zone as Influenced by Tillage*. 1966.

[9] D. H. Currence and W. G. Lovely, “The Analysis of Soil Surface Roughness,” *Trans. ASAE*, vol. 13, no. 6, pp. 0710–0714, 1970, doi: 10.13031/2013.38702.

[10] M. J. M. Römkens and J. Y. Wang, “Effect of Tillage on Surface Roughness,” *Trans. ASAE*, vol. 29, no. 2, pp. 0429–0433, 1986, doi: 10.13031/2013.30167.

[11] *DIN 4760:1982-06: Gestaltabweichungen; Begriffe, Ordnungssystem*, 4760, Jun. 1982. doi: https://dx.doi.org/10.31030/1110827.

[12] *DIN EN ISO 25178-2:2023-09, Geometrische Produktspezifikation (GPS) - Oberflächenbeschaffenheit: Flächenhaft - Teil 2: Begriffe und Kenngrößen für die Oberflächenbeschaffenheit (ISO 25178-2:2021); Deutsche Fassung EN ISO 25178-2:2022*. doi: 10.31030/3294021.

[13] *DIN EN ISO 21920-2:2022-12, Geometrische Produktspezifikation (GPS) - Oberflächenbeschaffenheit: Profile - Teil 2: Begriffe und Kenngrößen für die Oberflächenbeschaffenheit (ISO 21920-2:2021, korrigierte Fassung 2022-06); Deutsche Fassung EN ISO 21920-2:2022*. doi: 10.31030/3294017.

[14] F. Mohammadi, M. R. Maleki, and J. Khodaei, “Control of variable rate system of a rotary tiller based on real-time measurement of soil surface roughness,” *Soil Tillage Res.*, vol. 215, p. 105216, Jan. 2022, doi: 10.1016/j.still.2021.105216.

[15] A. Azizi, Y. Abbaspour-Gilandeh, T. Mesri-Gundoshmian, A. A. Farooque, and H. Afzaal, “Estimation of Soil Surface Roughness Using Stereo Vision Approach,” *Sensors*, vol. 21, no. 13, p. 4386, Jun. 2021, doi: 10.3390/s21134386.

[16] S. Steinhaus, *Methodik zur Bewertung und Erfassung der Effektivität und Effizienz von landwirtschaftlichen Verfahren und Prozessen*. in Forschungsberichte aus dem Institut für mobile Maschinen und Nutzfahrzeuge. Düren: Shaker Verlag, 2022.

[17] D. R. Linden and D. M. Van Doren, “Parameters for Characterizing Tillage-induced Soil Surface Roughness,” *Soil Sci. Soc. Am. J.*, vol. 50, no. 6, pp. 1560–1565, Nov. 1986, doi: 10.2136/sssaj1986.03615995005000060035x.

[18] J. Boiffin, “La dégradation structurale des couches superficielles du sol sous l’action des pluies,” Ph.D. dissertation, Institut National Agronomique Paris Grignon, 1984. [Online]. Available: https://hal.inrae.fr/tel-02858167

[19] P. Bertuzzi, G. Rauws, and D. Courault, “Testing roughness indices to estimate soil surface roughness changes due to simulated rainfall,” *Soil Tillage Res.*, vol. 17, no. 1–2, pp. 87–99, Aug. 1990, doi: 10.1016/0167-1987(90)90008-2.

[20] D. R. Linden, D. M. van Doren, and R. R. Allmaras, “A model of the effect of tillage-induced soil surface roughness on erosion,” vol. 1988. pp. 373–378, 1988.

[21] A. Martinez-Agirre, J. Álvarez-Mozos, and R. Giménez, “Evaluation of surface roughness parameters in agricultural soils with different tillage conditions using a laser profile meter,” *Soil Tillage Res.*, vol. 161, pp. 19–30, Jan. 2016, doi: 10.1016/j.still.2016.02.013.

[22] M. Graf, F. Fuchshumer, and M. Geimer, “Soil Tillage Quality Measurement: A Methodical Approach,” in *AgEng 2024 Proceedings Book*, 2024, p. 367. Accessed: Aug. 30, 2024. [Online]. Available: https://publikationen.bibliothek.kit.edu/1000173849

[23] U. Hillig, “Ermittlung der Gesetzmäßigkeit des Zerkleinerungsergebnisses durch ausgewählte Bodenbearbeitungswerkzeuge auf unterschiedlichen Standorten,” Ph.D. dissertation, TU Dresden, Dresden, 1986.

[24] R. Soucek, “Beiträge der Grundlagen- und angewandten Forschung zur Entwicklung von Bodenbearbeitungsgeräten und -maschinen,” Ph.D. dissertation, TU Dresden, Dresden, 1986.